PROCEEDINGS OF SCIENCE

Maximizing the time resolution of a particle counter with dead time

Flavia Gesualdi[a,b,*] **and Alberto Daniel Supanitsky**[a]

[a] *Instituto de Tecnologías en Detección y Astropartículas (CNEA, CONICET, UNSAM), San Martín, Argentina*

[b] *Karlsruhe Institute of Technology (KIT), Institute for Astroparticle Physics, Baden-Württemberg, Germany*

E-mail: flavia.gesualdi@iteda.cnea.gov.ar

We present a method for estimating the number of counts as a function of time of a counter with sub-units for which the expected count densities are the same. This is typically given in arrays of photo-multipliers in neutrino experiments, as well as in the segments of one segmented counter for indirect detection of cosmic rays. We take the latter as study case, and simulate and compare the performance of our algorithm in a detector like the Underground Muon Detector of the Pierre Auger Observatory. By properly accounting for the dead time of the counter, we provide estimates of the counts as a function of time to a single time-bin resolution.

38th International Cosmic Ray Conference (ICRC2023)
26 July - 3 August, 2023
Nagoya, Japan

*Speaker

PoS(ICRC2023)359

1. Introduction

In this work, we present a new, general method for counting particles that hit a counting detector with counting sub-units [1]. The method can be applied: (1) if the signal processing of each sub-unit is based on a discrimination threshold (rather than on the signal amplitude or charge) and is thus susceptible to the effect of unresolved particles, (2) if there is a subset (> 1) of counting sub-units that expect the same particle rate, and (3) if not all the sub-units of the subset have signal simultaneously (i.e. if there is no saturation). Even when individual particles cannot always be time-resolved, this method can be used for estimating particle counts as a function of time.

We find a clear case for applying our method in the Underground Muon Detector of the Pierre Auger Observatory [2]. Therefore we now discuss the significance of this method in the context of cosmic ray physics. We delay the discussion on other possible applications of the counting strategy, like neutrino experiments, to Sec. 5.

Despite extensive research, the origin of ultra high-energy cosmic rays (UHECRs) remains to be understood. To unravel this, cosmic rays are primarily investigated using three observables: the energy spectrum, the distribution of arrival directions, and the mass composition as a function of energy [3]. The depth of the shower maximum and the number of muons are two extensive air-shower (EAS) observables that are particularly sensitive to the mass composition [4]. Buried or shielded detectors are capable of detecting muons model-independently, as other EAS particles are largely absorbed by the earth or shielding material above the detector.

In this work we simulate a detector like the Underground Muon Detector (UMD) of the Pierre Auger Observatory and use it as a test base for comparing various counting methods. A UMD module has 64 plastic scintillator strips with wavelength-shifting optical fibers optically connected to silicon photo-multipliers (SiPMs) [2, 5].

2. Counting methods

Counting particles on a segmented detector can be compared to the statistical problem of counting "balls in boxes"[1]. In the latter, a finite number of balls (the particles) are randomly uniformly allocated in a finite number of boxes (the detector segments). After one realization, each box can contain 0 (with no pattern match), or ≥ 1 balls (with pattern match or occupied). The number of occupied boxes defines in this way the *occupancy*.

In a muon counter, the balls would represent the number of muons impinging on the counter N_μ. We assume that N_μ originates from one realization of a Poisson distribution with mean μ. The latter is the average number of particles expected on the counter. μ depends on the energy, primary mass, zenith angle, and distance to the shower axis. Notice the difference between N_μ and μ: N_μ is the number of particles actually impinging the detector, a property of the event, while μ is the average number, a property of the EASs. Both quantities, N_μ and μ, can be independently used to reconstruct the muon lateral distribution function [4, 7, 8].

There are two questions that the counting methods intend to address: (1) Knowing the occupancy, what is the estimated number of impinging particles, N_μ? (2) Assuming that N_μ is a realization of a Poisson distribution of mean μ, what is the estimated mean number of particles μ?

[1]This is also referred to as "classical shot problem" or "classical occupancy problem" [6].

The total number of pattern matches across all scintillator strips would be the simplest estimate of both N_μ and μ. However, it is obvious that the pile-up effect would bias the estimates, as one pattern match can account for multiple muons. Therefore, the objective of these counting methods is to offer a pile-up-unbiased estimate of N_μ and μ using the information from the event trace.

We now describe the four counting strategies considered in this work.

The **infinite window method** was the one utilized by the AGASA collaboration (see for example Ref. [9]). It is the simplest counting method in the sense that it does not use the temporal structure of the event trace. It only makes use of the number of occupied channels k (the occupancy), which is computed as [4, 7, 10]

$$k = \sum_{i=1}^{n_s} \Theta(m_i), \tag{1}$$

where n_s is the number of active segments of the detector, m_i is the number of pattern matches starting at the i-th channel, and Θ is the Heaviside step function ($\Theta(m_i) = 0$ if $m_i = 0$, else $\Theta(m_i) = 1$).

The number of muons impinging on a scintillator bar follows a Poisson distribution of mean μ/n_s (this is deducible just from the definition of μ). Therefore, the probability of a channel being empty is $q = \exp(-\mu/n_s)$, and the probability of a channel being occupied is $p = 1 - q$ [7, 8]. The probability of having k occupied channels (successes) out of n_s channels (trials) given μ (which determines the success probability) follows a binomial distribution $B(k|\,\mu) = \binom{n_s}{k} p^k q^{n_s-k} = \binom{n_s}{k} e^{-\mu}(e^{\mu/n_s} - 1)^k$ [7, 8]. This can also be seen as the likelihood of μ given k occupied channels. For $k < n_s$ (no saturation) the maximum likelihood estimator of μ is [7, 8]

$$\widehat{\mu} = -n_s \ln\left(1 - \frac{k}{n_s}\right). \tag{2}$$

Furthermore, the probability of k channels being occupied given N_μ impinging muons and n_s scintillation bars is given by the classical occupancy distribution $\mathrm{Occ}\,(k|\,N_\mu, n_s) = \binom{n_s}{k} \frac{S(N_\mu,k)}{n_s^{N_\mu}}\ \forall\, k \in \mathbb{Z} \mid 1 \le k \le n_s$ [10], where $S(N_\mu, k)$ are the Stirling numbers of the second kind (see also Ref. [6]). A good approximation of the maximum likelihood estimator of N_μ is (see Refs. [4, 10])

$$\widehat{N}_\mu = \ln\left(1 - \frac{k}{n_s}\right) \Big/ \ln\left(1 - \frac{1}{n_s}\right). \tag{3}$$

It is easy to see that Eq. (2) and Eq. (3) are very similar, and actually $\widehat{N}_\mu \to \widehat{\mu}$ when $n_s \to \infty$. The module is said to be saturated when $k = n_s$, and in that case both $\widehat{\mu}$ and $\widehat{N}_\mu$ tend to infinity.

The next tested method is the **N-bin window**. First introduced in Ref. [8], this method has been used for analyses of PMT data of the Auger UMD in Refs. [11, 12][2]. In this method, the detector trace is divided into time windows of N bins, where N is the number of bins of a single-muon pattern (in the case of SiPMs of the Auger UMD, N = 12 time-bins of 3.125 ns each). For each j-th window, the number of occupied channels k_j, the estimated number of muons $\widehat{N}_{\mu,j}$, and the estimated average number of muons $\widehat{\mu}_j$ are computed using Eqs. (1,2,3) respectively. Then the total

[2] We show in Sec. 4 that this counting method introduces significant biases. In the analyses of Refs. [11, 12], these are compensated for, at least to first order, by correcting them against simulations in a subsequent stage.

$\widehat{N}_\mu$ and $\widehat{\mu}$ are estimated from the sum over the window-wise estimates:

$$\widehat{N}_\mu = \sum_{j=1}^{n_w} \widehat{N}_{\mu,j}, \tag{4}$$

$$\widehat{\mu} = \sum_{j=1}^{n_w} \widehat{\mu}_j, \tag{5}$$

where j runs over the n_w number of windows of the trace.

Furthermore, we introduce the **N-bin centered window** method, only to enlighten the origin of biases in the N-bin method. It is fairly similar to the latter, but it positions the windows such that one of the windows has its center aligned with the signal peak. For simplicity, we explain the method using the case of the 12 time-bin windows corresponding to SiPMs of the Auger UMD. The idea is the following: We know that there exists at least one 12 time-bin window j^* in which the number of occupied channels k_j is maximum. If there is more than one window, we take the one that starts earliest. To find it, we slide a 12 time-bin window over all the trace, computing k_j for every j-th possible window. The "centered" window is the one that starts earliest such that $k_{j^*} = \max_j(k_j)$. This window determines the way to complete the partition of the trace into 12 time-bin windows. Having determined the way to partition the trace, $\widehat{N}_\mu$ and $\widehat{\mu}$ are computed as in Eqs. (4,5).

This leads us to the counting method that we developed, the **1-bin window**. This method makes use of the signal's entire temporal structure rather than using the trace as a whole or in many-bin windows. For this, we compute at each j-th time-bin of the trace, besides the number of occupied channels k_j, the number of inhibited channels $n_{\text{inhib},j}$. The latter represents the number of channels with a pattern match that started in a previous time-bin. We refer to these as inhibited channels because it would be impossible to resolve a muon if it fell within that time bin. In essence, inhibited channels are the same as dead channels. In the analogy of balls in boxes, channels that are occupied can be treated as having fewer available boxes. The number of non-inhibited channels is $n_s - n_{\text{inhib},j}$.

However, having less available (non-inhibited) channels reduces the detector area, which leads to a smaller number of detectable muons. The usable detector area varies with time. To obtain the number of muons that would be observed for a constant detector area equal to the active area, it is necessary to multiply by the number of active segments n_s and to divide by the number of non-inhibited segments $n_s - n_{\text{inhib},j}$. Therefore, we compute

$$\widehat{\mu}_j = \widehat{\mu}_j = -n_s \ln\left(1 - \frac{k_j}{n_s - n_{\text{inhib},j}}\right), \tag{6}$$

and

$$\widehat{N}_{\mu,j} = \frac{n_s}{n_s - n_{\text{inhib},j}} \times \ln\left(1 - \frac{k_j}{n_s - n_{\text{inhib},j}}\right) \Big/ \ln\left(1 - \frac{1}{n_s - n_{\text{inhib},j}}\right), \tag{7}$$

for each bin of the trace. The overall $\widehat{N}_\mu$ and $\widehat{\mu}$ are computed as their sum over all the bins of the trace (this is, as in Eqs. (4,5), with the number of windows n_w being equal to the number of bins in the trace).

3. Simulations

In an effort to reproduce a realistic scenario, we simulate the electronics response of the counter mode of the Auger UMD. The complete technical description can be found in Ref. [1]. The detector's model follows Ref. [13]. Based on this model, we derive an analytical solution for the detector response to one or more muons. We disregard electronic noise, which is irrelevant for evaluating the counting methods. It is also relevant to mention that we do not account for the effect of one muon being detected in two scintillator strips, because this effect is a separate source of bias that can be corrected afterwards [11]. Figure 1 shows the impinging muons, binary traces, and matched patterns, and applied 1-bin counting method for an example simulated module-level event. Only channels with signal are shown. We can find pile-up muons in channel 16.

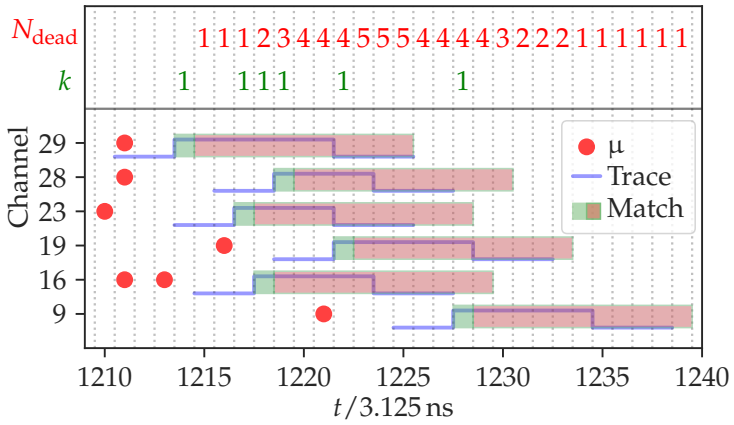

Figure 1: Example of a simulated signal in a UMD module. Muons (circles) impinge at a given time (x-axis) on the segments of the module, and in their corresponding channel (y-axis) we find a binary signal (lines). These are matched to a single-muon pattern (rectangles). The occupancy k and number of inhibited channels n_{inhib} at each time-bin illustrate how to apply the 1-bin counting method.

There are two detector effects that cause biases in $\widehat{N}_\mu$ and $\widehat{\mu}$, which are not related to pile-up, nor are intrinsic to the counting methods. The first one is a detector inefficiency, and it happens when a muon does not create a signal that matches the single-muon pattern. It causes undercounting in all methods to the same extent. In Ref. [1] we showed this effect is below 4 %.

The second source of bias is due to an undershoot in the electronics. It can happen that the signal of a later muon mounts on the undershoot of a previous one, such that the later muon is not matched to a single-muon pattern. The infinite window method is insensitive to this bias because it is enough to match the early muons in the channel to tag it as occupied during the whole trace. All other methods are sensitive to this effect to the same extent. The pattern matches lost due to undershoot can amount from 0.1 % for low-energetic, inclined air-showers, to 3.3 % for high-energetic, vertical air-showers, as proven in Ref. [1].

We generated a library of ~7600 EASs of proton and iron primaries, using EPOS-LHC [14] and UrQMD [15, 16] as high- and low-energy hadronic interaction models, respectively. The showers were generated using CORSIKA v7.7402 [17]. We used primary energies uniformly distributed in $17.2 \leq \log_{10}(E/\text{eV}) \leq 18.4$ and zenith angles in $0^\circ \leq \theta \leq 48^\circ$ corresponding to an isotropic distribution. Further details can be found in Ref. [1].

4. Results

Although the general behavior also applies to μ, we compare the performance of the different counting methods only for N_μ for the sake of simplicity. The difference is that the resolution in the estimation of μ is sensitive to Poissonian fluctuations in N_μ. When N_μ is significantly smaller than the total number of segments, these become dominant. In contrast, when N_μ is high, the detector segmentation predominates, resulting in identical resolutions for the estimators of N_μ and μ [7].

We define the relative difference between the estimated and input (or true) number of muons as $\varepsilon = (\widehat{N}_\mu - N_\mu)/N_\mu$.

Figure 2 shows the relative bias $\langle\varepsilon\rangle$ (left panel) and the relative resolution $\sigma(\varepsilon)$ (right panel) of each counting method. The error bars on the mean ε represent the standard deviation of the mean. The error bars of the standard deviation of ε were calculated using bootstrap. Compared to the other strategies, the N-bin strategy stands out for having a considerably larger relative bias (more negative) and larger standard deviation. Additionally, the N-bin centered, infinite window, and 1-bin strategies all perform roughly similarly in terms of mean relative bias: for an input of $N_\mu \lesssim 200$, they all have a small, mostly negative bias contained within $\pm 10\,\%$ that is dominated by detector effects, presenting an increasingly negative bias above that when the detector starts to saturate. For the N-bin and N-bin centered strategies $\langle\varepsilon\rangle$ tends to more negative values because of not considering inhibited channels. The 1-bin method behaves similarly to the infinite window method with a smaller detector, however because of the undershoot effect, it tends to slightly more negative values. The bias in the infinite window strategy is the smallest, yet it is not null. We notice that the 1-bin strategy's precision is roughly similar to or greater than that of the other strategies when we compare the standard deviations.

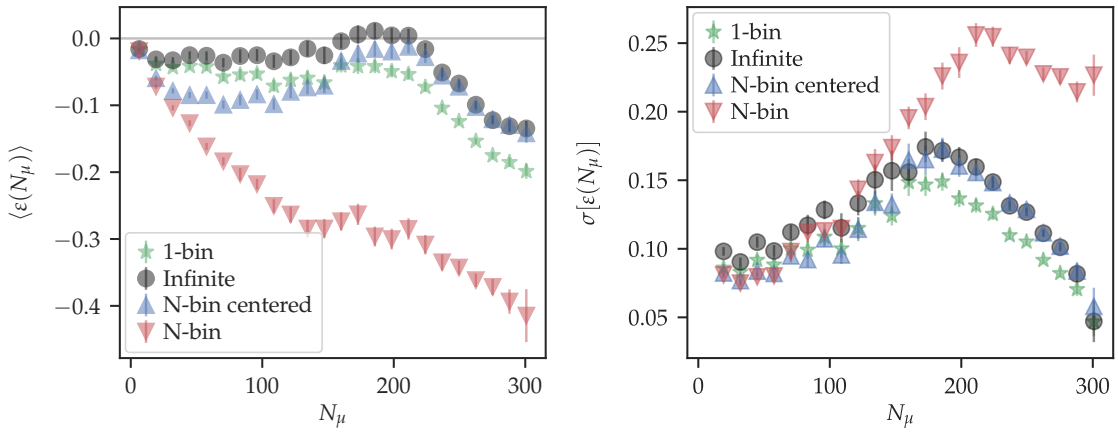

Figure 2: Relative bias (left) and relative standard deviation (right) in the reconstructed number of muons as a function of the input number of muons for the four counting methods considered.

As mentioned before, the 1-bin counting method developed in this work allows for the reconstruction of the muon time structure. Figure 3 shows an example of the impinging muons, the average input number of muons as seen by the detector, and the estimated average number of muons computed using the 1-bin strategy, all as a function of time. The input muons as a function of time correspond to the mean muon time structure of proton showers with $18.0 \leq \log_{10}(E/\mathrm{eV}) \leq 18.2$

and $\theta \lesssim 18^\circ$ ($\sin^2\theta \leq 0.10$) at 450 m from the core. Between the input muons and the muons seen by the detector there is a time delay, which amounts to the propagation of the photons in the optic fiber, and to the scintillator and optic fiber delays.

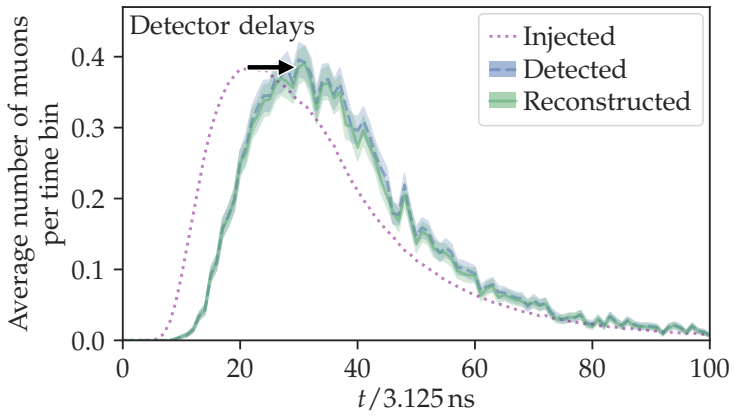

Figure 3: Input number of muons (dotted line), input number of muons as seen by the detector (dashed line), and reconstructed number of muons (solid line) using the 1-bin counting method, as a function of time. The input number of muons as a function of time is the mean muon time structure of proton showers with $18.0 \leq \log_{10}(E/\mathrm{eV}) \leq 18.2$ and $\theta \lesssim 18^\circ$ ($\sin^2\theta \leq 0.10$) at 450 m from the core. The mean number of muons as seen by the detector is computed by introducing the true time delays from the detector in the input muons. Shaded areas represent 1 σ uncertainties.

5. Summary and outlook

We presented and compared four counting methods that account for the pile-up effect: the infinite window, N-bin window, N-bin centered window, and the 1-bin method (developed in this work). All four methods are based on the solution to the classical occupancy or "balls-in-boxes" problem, where the particles are represented by balls and the segments of the detector by boxes. The strategies differ mainly in the duration of the window within which one realization of the balls-in-boxes problem is considered. The difference between the N-bin and N-bin centered strategies is that the position of the windows are determined such that the center of the output signal aligns with the center of a given window. What differentiates the 1-bin method from all others is the consideration of inhibited segments.

The muon counters of the Underground Muon Detector at the Pierre Auger Observatory provide a specific application for this general counting method. To test and compare the various methods, we used the latter as our research case. We demonstrated that all methods but the N-bin one perform well for typical time structures of the muon signal in a detector like the Auger UMD. The mean bias is contained within $\pm 10\,\%$ for all methods other than the N-bin one, provided that saturation is not significant.

Finally, we demonstrated that the 1-bin method may be used to reconstruct the time structure of the muon signal as observed by the detector down to a single time-bin resolution. Such a resolution is not provided by any other known method. This makes it possible to do novel research on the muon component's temporal structure. Such research could be key for mass composition analysis.

Finally, counting photons produced in liquid scintillators with photo-multiplier tubes (PMTs), a typical design of neutrino studies, may be possible using the counting method established in this work. The method is only useful if the PMT signals are processed using a discriminating threshold (counter mode). In this context, it is possible to determine the energy of the neutrino by counting the estimated number of scintillation photons produced in a neutrino event (e.g. as in Ref. [18]). More specifically, since the expected scintillation photon rate is the same for all sets of PMTs positioned equally apart from the interaction vertex, the proposed counting method may be used there. These sets would be rings in spherical detectors, corresponding to the intersection of spheres centered at the vertex with the larger spherical array of PMTs. This applies, for instance, to the Jiangmen Underground Neutrino Observatory (JUNO) [19] and the Sudbury Neutrino Observatory + (SNO+) [20]. The group of PMTs in cylindrical detectors that expect an identical rate would follow more complicated curves formed by the intersection of spheres centered at the vertex with the cylindrical array.

Acknowledgements The authors would like to thank Martin Schimassek for the presentation of the poster associated to this proceeding at the conference venue.

References

[1] Gesualdi, F., Supanitsky, A.D., Eur. Phys. J. C **82**, 925 (2022). https://doi.org/10.1140/epjc/s10052-022-10895-9
[2] A. Aab et al., J. Instrum. **16**(04), 04003 (2021). https://doi.org/10.1088/1748-0221/16/04/p04003
[3] S. Mollerach, J. Phys: Conf. Ser. 2156(1), 012007 (2021). https://doi.org/10.1088/1742-6596/2156/1/012007
[4] A.D. Supanitsky *et al.*, Astropart. Phys. **29**(6), 461–470 (2008). https://doi.org/10.1016/j.astropartphys.2008.05.003
[5] A. Aab et al., The Pierre Auger Observatory Upgrade - Preliminary Design Report (2016) arXiv:1604.03637
[6] B. O'Neill, Am. Stat. **75**(4), 364–375 (2020). https://doi.org/10.1080/00031305.2019.1699445
[7] D. Ravignani, A.D. Supanitsky, Astropart. Phys. **65** (2014). https://doi.org/10.1016/j.astropartphys.2014.11.007
[8] D. Ravignani, A.D. Supanitsky, D. Melo, Astropart. Phys. **82**, 108–116 (2016). https://doi.org/10.1016/j.astropartphys.2016.06.001
[9] N. Hayashida *et al.*, J. Phys. G: Nucl. Part. Phys. 21, 1101–1119 (1995).
[10] A.D. Supanitsky, Astropart. Phys. **127**, 102535 (2021). https://doi.org/10.1016/j.astropartphys.2020.102535
[11] S. Müller for the Pierre Auger Collaboration, EPJ Web Conf. 210, 02013 (2019). https://doi.org/10.1051/epjconf/201921002013
[12] A. Aab *et al.*,, Eur. Phys. J. C **80**(8), 751 (2020). https://doi.org/10.1140/epjc/s10052-020-8055-y
[13] A.M. Botti *et al.*,J. Instrum. 16(07), 07059 (2021). https://doi.org/10.1088/1748-0221/16/07/p07059
[14] T. Pierog *et al.*,Phys. Rev. C **92**(3), 034906 (2015). https://doi.org/10.1103/PhysRevC.92.034906.
[15] S.A. Bass *et al.*, Prog. Part. Nucl. Phys. **41**, 255–369 (1998). https://doi.org/10.1016/ S0146-6410(98)00058-1
[16] M. Bleicher *et al.*, J. Phys. G: Nucl. Part. Phys. **25**(9), 1859–1896 (1999). https://doi.org/10.1088/0954-3899/25/9/308
[17] D. Heck *et al.*, Technical report (1998). https://doi.org/10.5445/IR/270043064. 51.02.03; LK 01; Wissenschaftliche Berichte, FZKA-6019 (Februar 98)
[18] W. Wu *et al.*,J. Instrum. **14**(03), 03009–03009 (2019). https://doi.org/10.1088/1748-0221/14/03/p03009
[19] A. Abusleme *et al.*, Prog. Part. Nucl. Phys. **123**, 103927 (2022). https://doi.org/10.1016/j.ppnp.2021.103927
[20] S. Andringa *et al.*, Adv. High Energy Phys. **2016** (2016). https://doi.org/10.1155/2016/6194250.